



RESEARCH PAPER

 OPEN ACCESS



## Conserved small mRNA with an unique, extended Shine-Dalgarno sequence

Julia Hahn<sup>a</sup>, Sebastian Thalmann <sup>a</sup>, Anzhela Migur<sup>a,b</sup>, Raphael Freiherr von Boeselager<sup>c</sup>, Nina Kubatova<sup>d</sup>, Elena Kubareva<sup>b</sup>, Harald Schwalbe<sup>d</sup>, and Elena Evguenieva-Hackenberg <sup>a</sup>

<sup>a</sup>Institute of Microbiology and Molecular Biology, Justus-Liebig-University, Gießen, Germany; <sup>b</sup>A.N. Belozersky Institute of Physico-Chemical Biology, M.V. Lomonosov Moscow State University, Leninsky Gory 1, Moscow, Russia; <sup>c</sup>Institut für Bio- und Geowissenschaften, IBG-1: Biotechnologie, Forschungszentrum Jülich, Germany; <sup>d</sup>Institut für Organische Chemie und Chemische Biologie, Center for Biomolecular Magnetic Resonance (BMRZ), Johann Wolfgang Goethe-Universität, Frankfurt am Main, Germany

### ABSTRACT

Up to now, very small protein-coding genes have remained unrecognized in sequenced genomes. We identified an mRNA of 165 nucleotides (nt), which is conserved in *Bradyrhizobiaceae* and encodes a polypeptide with 14 amino acid residues (aa). The small mRNA harboring a unique Shine-Dalgarno sequence (SD) with a length of 17 nt was localized predominantly in the ribosome-containing P100 fraction of *Bradyrhizobium japonicum* USDA 110. Strong interaction between the mRNA and 30S ribosomal subunits was demonstrated by their co-sedimentation in sucrose density gradient. Using translational fusions with *egfp*, we detected weak translation and found that it is impeded by both the extended SD and the GTG start codon (instead of ATG). Biophysical characterization (CD- and NMR-spectroscopy) showed that synthesized polypeptide remained unstructured in physiological puffer. Replacement of the start codon by a stop codon increased the stability of the transcript, strongly suggesting additional posttranscriptional regulation at the ribosome. Therefore, the small gene was named *rreB* (ribosome-regulated expression in *Bradyrhizobiaceae*). Assuming that the unique ribosome binding site (RBS) is a hallmark of *rreB* homologs or similarly regulated genes, we looked for similar putative RBS in bacterial genomes and detected regions with at least 16 nt complementarity to the 3'-end of 16S rRNA upstream of sORFs in *Caulobacteriales*, *Rhizobiales*, *Rhodobacterales* and *Rhodospirillales*. In the *Rhodobacter/Roseobacter* lineage of  $\alpha$ -proteobacteria the corresponding gene (*rreR*) is conserved and encodes an 18 aa protein. This shows how specific RBS features can be used to identify new genes with presumably similar control of expression at the RNA level.

### ARTICLE HISTORY

Received 6 September 2016  
Revised 19 October 2016  
Accepted 30 October 2016

### KEYWORDS

$\alpha$ -proteobacteria;  
*Bradyrhizobium*; ribosomal binding site; ribosome; RNA stability; Shine-Dalgarno; small gene; small protein; sORF; translation initiation region

## Introduction


Deep sequencing of bacterial transcriptomes revealed many non-annotated small transcripts, some of which are probably regulatory non-coding RNAs (sRNAs), small mRNAs, or RNAs with dual functions.<sup>1–4</sup> Most bacterial mRNAs harbor Shine-Dalgarno sequences (SDs) in their 5'-untranslated regions (5'-UTRs), which mediate the interaction of the mRNAs with the 30S ribosomal subunit.<sup>5,6</sup> Thus, the identification of canonical SDs should be helpful for identification of small functional open reading frames (sORFs) that are ignored in genome annotations.<sup>3,7</sup>

A canonical SD is located 5 to 9 nucleotides (nt) upstream of the translation initiation codon and has the sequence 5'-AGGAGG-3' that is perfectly complementary to the 3'-end of 16S rRNA.<sup>5,6</sup> However, most SDs are not perfectly complementary to 16S rRNA and canonical 6-meric SDs are strongly underrepresented in bacterial genomes.<sup>6</sup> Moreover, SDs longer than 6 nt with perfect complementarity to 16S rRNA have rarely been described. An extended SD consisting of 8 nt was shown to enable translation of a chloroplast mRNA from a

downstream GUG start codon instead of an upstream AUG codon.<sup>8</sup> Further, artificially extended SDs of 8 and 10 nt resulted in lower translation efficiency in *E. coli*, probably due to extraordinary strong binding to the anti-Shine-Dalgarno (aSD) in 16S rRNA, thus impeding transition from initiation to elongation of translation.<sup>9</sup> However, in another study with *E. coli* an 8 nt SD led to higher translation efficiency than SDs of 6 nt or 4 nt.<sup>10</sup>

Identification of small protein-encoding genes has remained a challenge, but examples of small proteins that fulfill important functions underline the importance of this research field.<sup>3,7,11</sup> Among others, small proteins influence resistance to antibiotics, regulate bacterial communication, or act as non-secreted toxins contributing to formation of persister cells.<sup>12–16</sup> Recently we re-annotated the genome of the *Bradyrhizobium japonicum* USDA 110, a soil-dwelling bacterium capable of fixing molecular nitrogen in symbiosis with several legume plants including soybean.<sup>17,18</sup> This re-annotation added 1,391 potential ORFs to the 8,317 originally annotated genes.<sup>19,20</sup> Although sORFs shorter than 30

**CONTACT** Elena Evguenieva-Hackenberg  [Elena.Evguenieva-Hackenberg@mikro.bio.uni-giessen.de](mailto:Elena.Evguenieva-Hackenberg@mikro.bio.uni-giessen.de)

 Supplemental data for this article can be accessed on the publisher's website.

Published with license by Taylor & Francis Group, LLC © Julia Hahn, Sebastian Thalmann, Anzhela Migur, Raphael Freiherr von Boeselager, Nina Kubatova, Elena Kubareva, Harald Schwalbe, and Elena Evguenieva-Hackenberg

This is an Open Access article distributed under the terms of the Creative Commons Attribution-NonCommercial-NoDerivatives License (<http://creativecommons.org/licenses/by-nc-nd/4.0/>), which permits non-commercial re-use, distribution, and reproduction in any medium, provided the original work is properly cited, and is not altered, transformed, or built upon in any way.

codons were not annotated, it is conceivable that such sORFs remain to be identified and that some of them are encoded by putative sRNAs. Many transcription start sites (TSSs) of orphan genes that may correspond to sRNAs or small mRNAs were recently mapped in the genome of *B. japonicum* USDA 110.<sup>19</sup>

In this work, we analyzed a small RNA in *B. japonicum* USDA 110 and found that it is an mRNA conserved in *Bradyrhizobium diazoefficiens*. It encodes a polypeptide chain comprising 14 amino acid residues (aa) and harbors an extremely large SD of 17 nt, which extends to a GTG start codon. The polypeptide chain, synthesized by solid-phase chemical synthesis, does not adopt a persistent secondary or tertiary structure as judged by CD- and NMR-spectroscopic analyses. We show that the unique ribosome binding site (RBS) is responsible for strong interaction with ribosomes and low translation efficiency. Furthermore, our data indicate ribosome-dependent degradation of the small mRNA. Thus, the corresponding gene was named *rreB* (ribose-regulated expression in *Bradyrhizobium*). Small genes with similar RBS, which are probably regulated at the RNA level in a similar way, were also found in other  $\alpha$ -proteobacteria.

## Experimental procedures

### Cultivation methods and cloning procedures

*B. japonicum* 110*spc4*, a spectinomycin-resistant derivative of *B. japonicum* USDA 110 (recently re-named to *Bradyrhizobium diazoefficiens*), was grown in PSY medium in the presence of spectinomycin at a concentration of 100  $\mu\text{g ml}^{-1}$  at 30°C.<sup>21-23</sup> *Escherichia coli* JM109 and *E. coli* S17-1 were cultivated in LB medium.<sup>24,25</sup> Standard cloning procedures were used.<sup>26</sup> Suitable constructs for ectopic expression in *B. japonicum* were cloned in pME3535XhoI or its derivatives, cleaved out with EcoRI and XhoI restriction endonucleases and re-cloned into the broad host range plasmid pRK290XhoI resulting in pJH-plasmids (see Table S1).<sup>27,28</sup> Additionally, the chromosome integration plasmid pRJpaph-gfp\_a1 was used.<sup>29</sup> The *gfp* gene of this plasmid was cleaved out with SpeI and KpnI and was replaced by a sequence containing BamHI, PstI and SphI restriction sites. The resulting plasmid pRJpaph-MCS was used to clone *rreB* derivatives. Plasmids were transferred from *E. coli* S17-1 to *B. japonicum* 110*spc4* by biparental conjugation.<sup>25</sup> Used plasmids and oligonucleotides are listed in Tables S1 and S2, respectively.

### RNA isolation and analysis

Total RNA was isolated with hot-phenol.<sup>30</sup> Soybean nodules were kindly provided by H.M. Fischer (ETH Zürich). RNA separation in urea-containing 10 % polyacrylamide gels, staining with ethidium bromide, semidry blotting, hybridization with radioactively labeled oligonucleotide probes, re-hybridization, signal detection and quantification were performed as described.<sup>31</sup> Oligonucleotides used for hybridization are listed in Table S2. RNA stability measurements after stop of transcription with rifampicin were performed as previously described.<sup>32</sup>

### Fractionation of cell-free extracts

*B. japonicum* cells were harvested by centrifugation at 13,000 g at 4°C, re-suspended in a buffer containing 20 mM HEPES-

KOH (pH 7.8), 10 mM MgCl<sub>2</sub> and 100 mM NaCl, and lysed by sonication. S100 and P100 fractions were obtained after ultracentrifugation at 100,000 g. RNA isolated from the S100 fraction and the P100 fraction was dissolved in the same volume and same volumes were analyzed by Northern blot hybridization. The P100 fraction was resuspended in the same buffer and further fractionated in 10 ml 5% to 40% sucrose density gradient containing 3 mM MgCl<sub>2</sub> at 75,000 g and 4°C for 16 h. Fractions (0.5 ml) were harvested from the top and absorption at 260 nm was measured to localize the 30S and 50S ribosomal subunits.<sup>33</sup>

### Western blot analysis

Exponentially growing *B. japonicum* cells were harvested and adjusted to an OD<sub>600</sub> of 10 in SDS-containing loading buffer. Cells were lysed by incubation at 100°C for 5 min, proteins were separated by SDS-PAGE and blotted onto a nitrocellulose membrane.<sup>26</sup> If necessary, cell suspensions were diluted tenfold prior to lysis. Detection was performed with GFP-specific antibodies (Clontech), Anti-Mouse IgG-Alkaline Phosphatase (Sigma) and CDP-Star (Roche). Signals were visualized using a chemiluminescence imager (Fusion SL4, Vilber).

### Flow cytometry and cell sorting

Flow cytometry analysis and cell sorting experiments were performed with a FACSAria II flow cytometer (Becton Dickinson, Heidelberg, Germany). For excitation, a blue solid-state laser with a wavelength of 488 nm was used. Forward-scatter characteristics (FSC) and side-scatter characteristics (SSC) were detected as small-angle and orthogonal scatter of the 488-nm laser. For the detection of EGFP fluorescence a 502 nm long-pass and a 530/30 nm band-pass filter set was used. The FACS-Diva software 6.0 was used for measurement and data recording. Tracking beads labeled with a mixture of fluorochromes (BD, Heidelberg, Germany) were used for the cytometer set-up and performance tracking. Noise was removed by thresholding on FSC and SSC, while cell size was discriminated over the intensity of the FSC signal. Four-way purity was used as the precision mode for cell sorting with a threshold rate of up to 8000 events/sec. Data were analyzed using FlowJo V10 (Tree Star, Ashland, USA).

### Peptide synthesis, CD and NMR analyses

The small polypeptides *rreB* from *B. japonicum* USDA 110 (14 aa) and *rreR* from *Dinoroseobacter shibae* DFL 12 (18 aa) were synthesized using standard Fmoc-chemistry and purified by reversed-phase HPLC. The purity of the synthesized products characterized by matrix-assisted laser desorption/ionization (MALDI) mass analysis was analytical HPLC and greater 95% for both peptides. Secondary structure analysis was performed by 1D <sup>1</sup>H-NMR experiments and circular dichroism (CD) spectroscopy (see Supplementary Methods).

### Bioinformatic analyses

Homologs of *rreB* were identified by BLASTN and were used for multiple sequence alignments and secondary structure prediction.<sup>34,35</sup> Clustal W was also used for multiple sequence alignments.<sup>36</sup> Phyre2 was used for prediction of structures of proteins.<sup>37</sup>

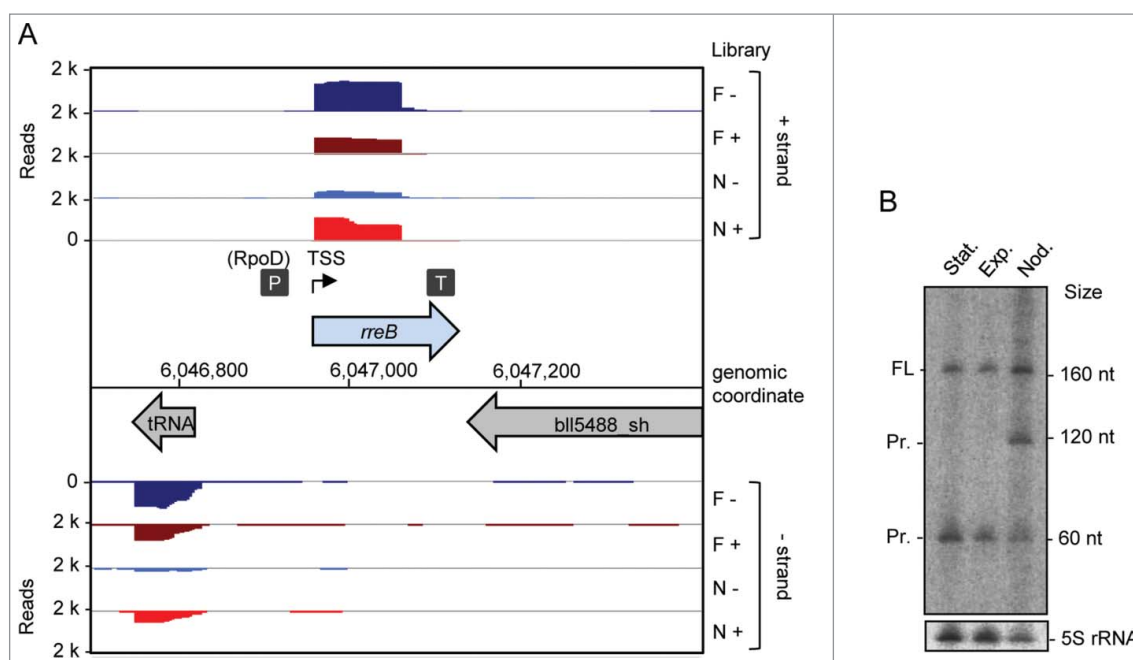


**Figure 1.** Detection of the small mRNA *rreB*. (A) Genomic context of *rreB* and cDNA reads, which originate from a previous differential RNA-seq analysis.<sup>19</sup> RNA was isolated from exponentially growing, free-living cells in liquid cultures (F) and from nodules (N). RNA samples were treated (+) or not treated (–) with terminal exonuclease (TEX), which degrades 5′-monophosphorylated (processed) transcripts. The scale of each library is indicated (Reads). Flexed thin black arrow, mapped TSS; dark gray boxes with P and T, mapped putative promoter and terminator, respectively.<sup>19</sup> The gene *rreB* is located between *Bj*at37 encoding tRNA-Gly and *blI5488\_sh* encoding a 2-component hybrid sensor and regulator. (B) Northern blot hybridization for detection of the sRNA *rreB* using a probe complementary to the sORF (see Fig. 2A). Total RNA isolated from liquid cultures grown to the exponential growth phase (Exp), the stationary phase (Stat) and from soybean nodules (Nod) was used. On the right side, the positions of the marker RNAs (160 nt, 120 nt and 60 nt corresponding to 6S rRNA, 5S rRNA and a fragment detected by the 6S RNA-specific probe, respectively<sup>30</sup>), are given. The full-length transcript (FL) and putative degradation products (Pr.) were detected. 5S rRNA was used as loading control.

## Results

### A small mRNA with extraordinarily long Shine-Dalgarno sequence in *Bradyrhizobiaceae*

Based on existing transcriptome data and previously mapped TSSs, promoters, and terminators, we identified a sRNA with a length of 165 nt, a TSS located at genomic position 6,046,962 and a putative RpoD-like promoter (Fig. 1A).<sup>19</sup> Northern blot analysis confirmed this transcript in exponentially growing and stationary free-living *B. japonicum* cells, and in symbiosis with soybean (Fig. 1B). In addition to the expected band of approximately 165 nt, the Northern blot analysis revealed a putative degradation product of approximately 120 nt present only in symbiosis and a putative degradation product of approximately 60 nt under all tested conditions (Fig. 1B).

The small RNA contains a sORF encoding a polypeptide chain (referred to here as small protein) of 14 aa. Interestingly, the SD upstream of the sORF is a part of a 17 nt region showing perfect complementarity to the 3′-end of 16S rRNA (17 nt complementarity-region or 17c-region; Fig. 2A). The complementarity region encompasses bases upstream and downstream of the canonical SD and includes the first base of the GTG start codon. Such an unprecedented SD extension should lead to a very strong binding of the small mRNA to 16S rRNA in the 30S ribosomal subunit and may negatively influence or even abolish translation of the small protein.<sup>9</sup> BLASTN analyses revealed that the small mRNA is conserved in the family *Bradyrhizobiaceae* (Fig. 2A and Fig. S1). The corresponding gene was named *rreB* (ribosome-regulated expression in *Bradyrhizobiaceae*; see below).

The small protein encoded by *rreB* is conserved (Fig. 2B and Fig. S1) and has predicted  $\alpha$ -helix and random coil regions (Fig. 2C). It was synthesized by standard Fmoc-chemistry and its structure was analyzed by CD and 1D-NMR spectroscopy (Figs. S2 to S5). However, the small protein RreB remained unstructured under all tested conditions, suggesting that it may adopt a structure only upon binding to interaction partner(s).

### The small mRNA *rreB* binds to the 30S ribosomal subunit

The presence of *rreB* homologs in several *Bradyrhizobiaceae* genera allowed prediction of a conserved secondary structure of the small mRNA. The prediction suggests that with exception of the 5 most upstream nucleotides, the 17c-region and the GTG start codon are involved in a double-stranded structure (Fig. 2C). The putative formation of double-stranded mRNA structure raised the question whether the 5′-UTR of *rreB* is accessible for interaction with ribosomes. To test whether *rreB* is bound to ribosomes, lysates of exponentially growing *B. japonicum* cultures were fractionated by ultracentrifugation at 100,000 g in supernatant (S100) fraction containing the soluble components of the cell and pellet (P100) fraction containing membranes and ribosomes. RNA from both fractions was analyzed by Northern blot hybridization along with total RNA.

The Northern blot analysis was performed with 3 probes directed to the 17c-region, the sORF (the same probe was used in Fig. 1B) and the 3′-UTR, respectively (Fig. 3A). As expected, with the sORF probe the 165 nt full-length *rreB* mRNA and the 60 nt degradation product were detected in

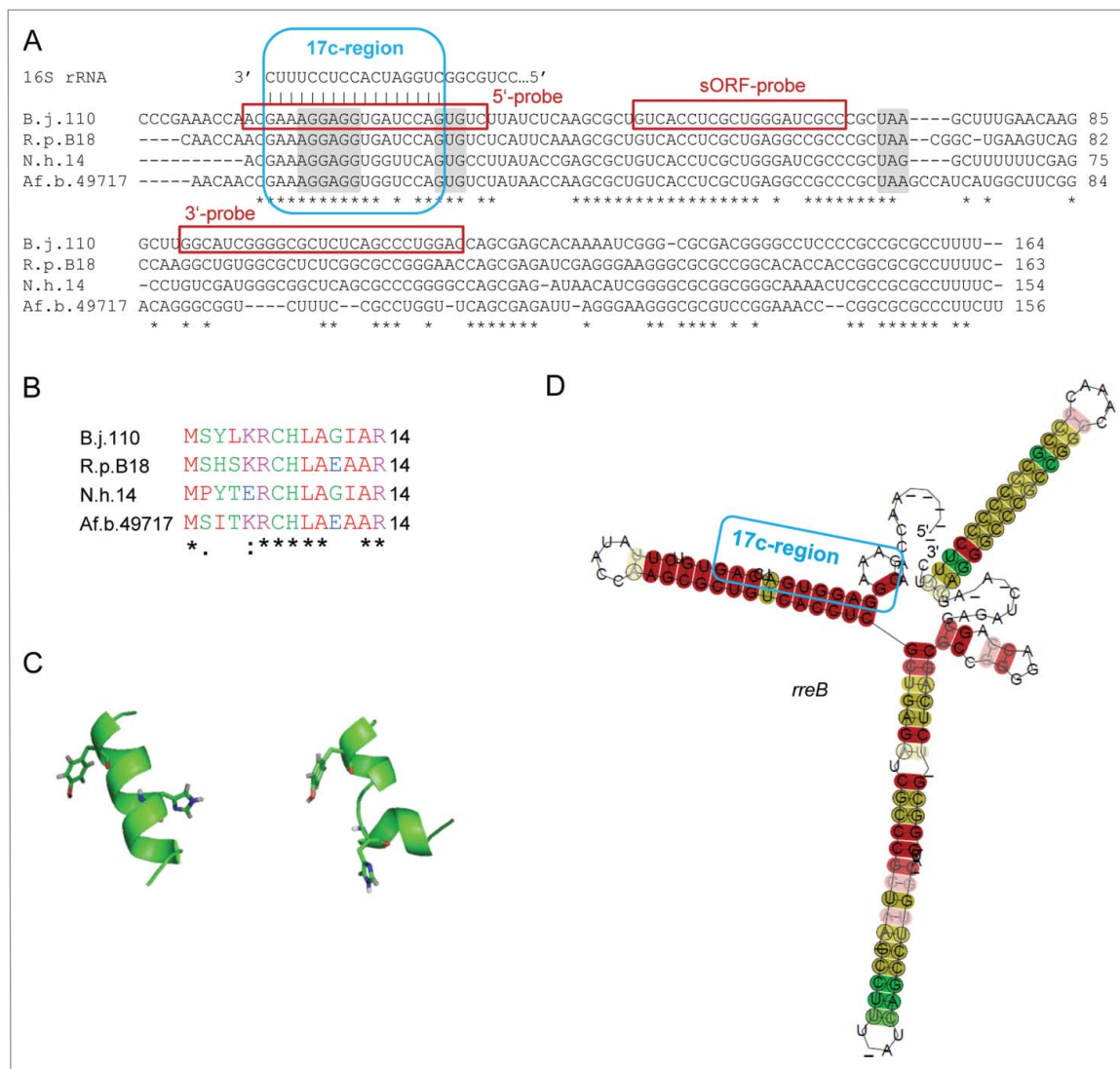


**Figure 2.** The conserved small RNA *rreB* contains a sORF and shows extended complementarity to the 3'-end of 16S rRNA. (A) Multiple sequence alignment of *rreB* mRNA and its homologs in 4 genera of *Bradyrhizobiaceae*. Asterisks mark invariant positions. The canonical SD sequence 5'-AGGAGG-3', the GUG start codon and UAA or UAG stop codons are highlighted. The sequence of the 3'-end of 16S rRNA is shown on the top. The 17 nt region of perfect complementarity between *rreB* and 16S rRNA (17c-region) is framed in blue. Sequences targeted by 3 different probes in Northern blot hybridizations are framed in red (see Fig. 3 below). B.j.110, *B. japonicum* USDA 110; R.p. B18, *Rhodopseudomonas palustris* BisB18; N.h. 14, *Nitrobacter hamburgensis* X14; Af. b. 49717, *Afipia broomeae* ATCC 49717. An extended alignment is shown in Fig. S1. (B) Multiple sequence alignment of the small proteins RreB encoded by the sORFs presented in A). An extended alignment is shown in Fig. S1. (C) Predicted spatial structure of RreB from *B. japonicum* USDA 110. Aromatic amino acid residues are marked. (D) Predicted RNA secondary structure of the *rreB* homologs shown in A). The LocARNA color annotation shows the conservation of base pairs - highly reliable prediction is indicated by the red color.<sup>36</sup> Less conserved basepairs are indicated by grey letters.

total RNA. In contrast, the 60 nt band was not detected with probes directed to the 5'- and 3'-UTR, respectively (Fig. 3A). After 100.000 g fractionation, the 60 nt band was detected predominantly in the S100 fraction, while the 165 nt band was mainly in the P100 fraction (Fig. 3A). As control for successful fractionation we used tRNA-Arg (Bjat49) which is not expected to be fully associated with ribosomes and was mainly in the S100 fraction, and 5S rRNA, which as part of the 50S ribosomal subunit was mainly in the P100 fraction (Fig. 3B). Thus, in contrast to the 60 nt processing product, most of the full-length *rreB* mRNA seemed to be associated with ribosomes.

The P100 fraction was further analyzed by ultracentrifugation in sucrose density gradients in which the ribosomal subunits were essentially separated (Fig. 3C and 3D). Twenty-two fractions were collected from the top of the gradient and RNA

was isolated from the peak fractions 3 (containing mRNAs and tRNAs), 10 (containing the 30S ribosomal subunit) and 14 (containing mainly the 50S ribosomal subunit; see Fig. 3C and 3D). Using Northern blot hybridization we detected the 165 nt *rreB* band in fraction 10 and the 60 nt *rreB* band in fraction 3 (Fig. 3E). As expected, the tRNA-Arg was in fraction 3 and 5S rRNA in fraction 14 (Fig. 3E). These results suggest that the 60 nt degradation product easily dissociates from the ribosomes, and show that full-length *rreB* mRNA is strongly bound to the 30S ribosomal subunit.

#### The 5'-extension of the SD is crucial for predominant localization of *rreB* at ribosomes

To analyze the impact of the 17c-region on the binding to ribosomes, we ectopically overexpressed 3 5'-truncated *rreB* mRNA

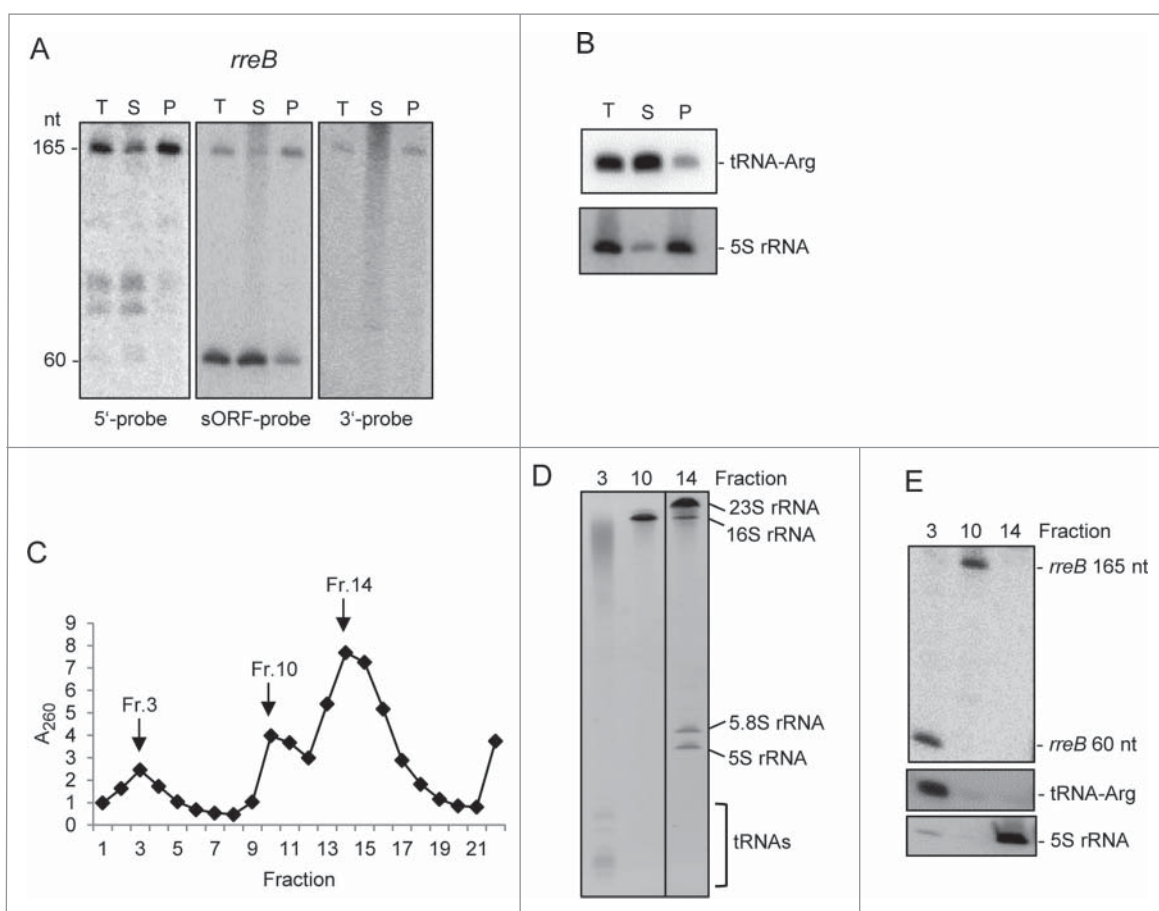


**Figure 3.** The small mRNA *rreB* is in the insoluble fraction and is strongly bound to the 30S ribosomal subunit in *B. japonicum*. (A) Northern blot analysis of total RNA (T) and RNA isolated from the P100 (P) and S100 (S) fraction using probes directed against the 5'-UTR (5'-probe), the sORF (ORF-probe) and the 3'-UTR (3'-probe) of *rreB* as indicated; the same membrane was re-hybridized. Main bands of approximately 165 nt and 60 nt were detected (marked at the left side). Their lengths were estimated by hybridization of the membrane with probes directed against the length standards 6S rRNA (160 nt), 5S rRNA (120 nt) and tRNA-Arg (79 nt) (not shown). (B) Northern blot analysis of tRNA-Arg and 5S rRNA. The membrane shown in A) was re-hybridized. (C) Separation of the P100 fraction through a 5% to 40% sucrose density gradient. The absorption of the gradient fractions at 260 nm is shown. Fractions which were further analyzed are marked with arrows. (D) Analysis of RNA isolated from fractions 3, 10 and 14 of the sucrose density gradient by electrophoresis. RNA was separated in urea-containing 10% polyacrylamide gel and stained with ethidium bromide (shown is a negative image). Distinct bands corresponding to the large 23S rRNA fragment (23S rRNA), 16S rRNA, the 5.8S rRNA-like short 5'-fragment of 23S rRNA, 5S rRNA and tRNAs are indicated. Fragmentation of 23S rRNA in *Bradyrhizobium japonicum* was described previously.<sup>40,41</sup> (E) Northern blot hybridization of RNA from the indicated sucrose density gradient fractions with probes directed against the sORF of *rreB*, tRNA-Arg and 5S rRNA.

derivatives (Fig. 4A): 1) *17c-rreB* lacking the first 8 nt of wild type *rreB* but still having the 17 nt complementary to 16S rRNA (compare Fig. 4A to Fig. 2A), 2) *14c-rreB* starting with the full canonical SD and having 14 nt complementary to 16S rRNA, and 3) *8c-rreB* lacking the canonical SD and having 8 nt complementary to 16S rRNA. When compared with endogenous *rreB*, the overexpression of the truncated *rreB* derivatives was strong in *B. japonicum*, ranging from 20-fold for *17c-rreB* to 120-fold for *8c-rreB*, as determined by Northern blot hybridization (Fig. 4B). The overexpressing strains were subjected to S100 and P100 fractionation followed by Northern blot hybridization, showing that *17c-rreB* was predominantly in the P100 fraction and the other 2 *rreB* derivatives with shortened region of complementarity to 16S rRNA were mainly in the S100 fraction (Fig. 4C). The strong difference in the localization of *17c-rreB* and *14c-rreB* shows that the most upstream nucleotides of the 17c-region are crucial for the predominant localization of *rreB* in P100 and thus for binding to ribosomes in *B. japonicum*. When analyzed in *E. coli*, the *rreB* derivatives accumulated to very low levels and were mainly in the S100 fraction (Fig. S6). To test whether 20-fold overproduction of

*17c-rreB* mRNA that tightly binds to ribosomes influences *B. japonicum* growth, growth curves of the overexpressing strain and the EVC were compared but no difference was found (not shown).

### The RBS of *rreB* suppresses translation

The strong binding of *rreB* to 16S rRNA may negatively influence translation.<sup>9</sup> To test whether translation of *rreB* takes place in *B. japonicum*, we cloned *rreB-egfp* translational fusions. For this purpose first a control plasmid pJH-F2 was created, which contains the *B. japonicum* *rrn* promoter, a 5'-UTR with a standard SD and an ATG start codon (standard RBS) from the bacterial overexpressing vector pQE30 (Qiagen), in frame *egfp*, and the *B. japonicum* *rrn* terminator. Plasmid pJH-F2 leads to strong *egfp* expression in *B. japonicum* (Fig. 5B, lane 2). Suitable restriction sites were included in pJH-F2 in order to enable construction of *egfp* translational fusions by replacement of the standard RBS (Fig. 5A).

To test the influence of the 17c-region on translation, we aimed to replace the standard RBS by the full *rreB* 5'-UTR and

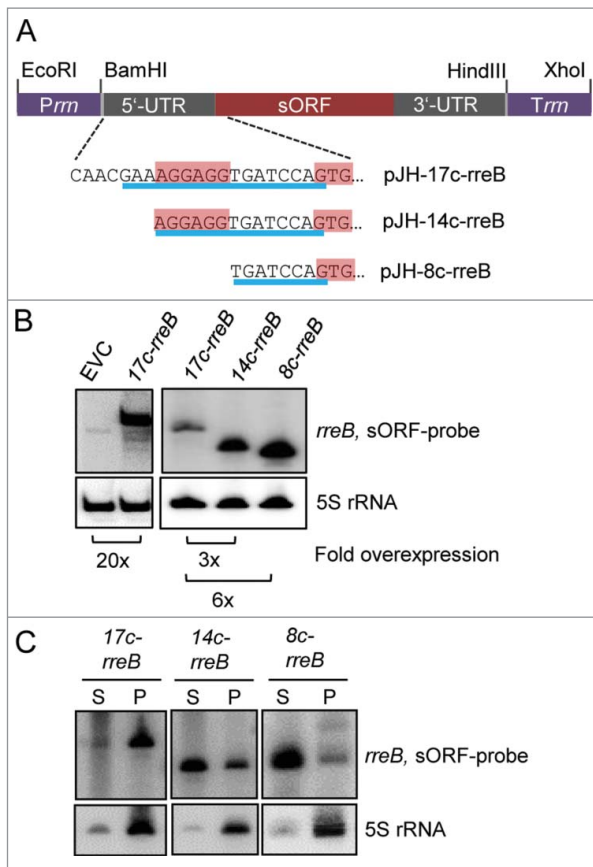


**Figure 4.** The 5'-nucleotides of the 17c-region are crucial for the predominant localization of *rreB* in the P100 fraction. (A) Schematic representation of the used constructs. The 5'-UTRs and GTG start codons of the *rreB* derivatives overexpressed from plasmids pJH-17c-rreB, pJH-14c-rreB, and pJH-8c-rreB are shown. The region of complementarity to 16S rRNA is underlined in blue. The canonical SD and the GTG start codon are highlighted. *Prrm*, rRNA (*rrn*) promoter; *Trm*, *rrn* terminator. (B) Northern blot hybridization of total RNA of *B. japonicum* strains overproducing the indicated *rreB* derivatives. EVC, empty vector control. (C) Northern blot hybridization of RNA isolated from the P100 (P) and S100 (S) fractions of strains overproducing the indicated *rreB* derivatives. (B) and (C) shown results from representative experiments. In each case, 3 independent biological experiments with similar results were performed. Probes directed against *rreB* and the 5S rRNA control were used.

the GTG start codon, but we failed to clone such a construct (marked with n.c. in Fig. 5A). Therefore, we cloned truncated derivatives with 14, 11 and 8 nt complementarity to 16S rRNA (pJH-14c-egfp, pJH-11c-egfp and pJH-8c-egfp; Fig. 5A). EGFP production in *B. japonicum* cells was monitored by Western blot analysis with GFP-specific antibodies (Fig. 5B). Signals corresponding to EGFP (33 kDa) were detected only in lysates with pJH-14c-egfp (lane 4) and the positive control pJH-F2 (lane 2). The EGFP signal in lane 4 was much weaker than that in lane 2 (consider the bottom panel which shows the loaded protein amounts in Fig. 5B). Thus, the RBS with the 14c-region supports weak translation, while the truncated 11c- and 8c-derivatives (lanes 5 and 6 in Fig. 5B) do not support it. Considering the strong overproduction of 14c-rreB mRNA (Fig. 4B) and the fact that its truncated 5'-UTR supports translation (Fig. 5B), we tested whether the increased RreB level influences growth. However, we did not find difference between the growth of *B. japonicum* (pJH-14c-rreB) and the EVC (not shown).

To analyze the impact of the full-length 5'-UTR of *rreB* on translation, we cloned the 5'-UTR together with the sORF in a translational fusion with *egfp*. Western blot analysis of cultures from cells containing the resulting plasmid pJH-17c-rreB-egfp revealed the presence of very low amounts of degraded EGFP (Fig. S7). Therefore we re-cloned the 17c-rreB-egfp construct to obtain a chromosome-integrating plasmid pRJ-17c-rreB-egfp, in which, the *rreB-egfp* translational fusion is under the control of a constitutive *Paph* promoter (Fig. 6A).<sup>29</sup> As a corresponding control pRJ-sSD-rreB-egfp was created, in which the standard RBS precedes the *rreB-egfp* fusion (Fig. 6A). The Western blot analysis in Fig. 6B shows that cells harboring pRJ-17c-rreB-egfp the fusion protein RreB-EGFP. The RreB-EGFP band from those cells was very weak when compared with the positive control with pRJ-sSD-rreB-egfp (compare lanes 4 and 5 in Fig. 6B considering the loaded protein amounts), in line with weak RreB-EGFP translation due to the 17c-region.

*B. japonicum* cells with the constructs shown in Fig. 6A were also examined under the fluorescence microscope. While

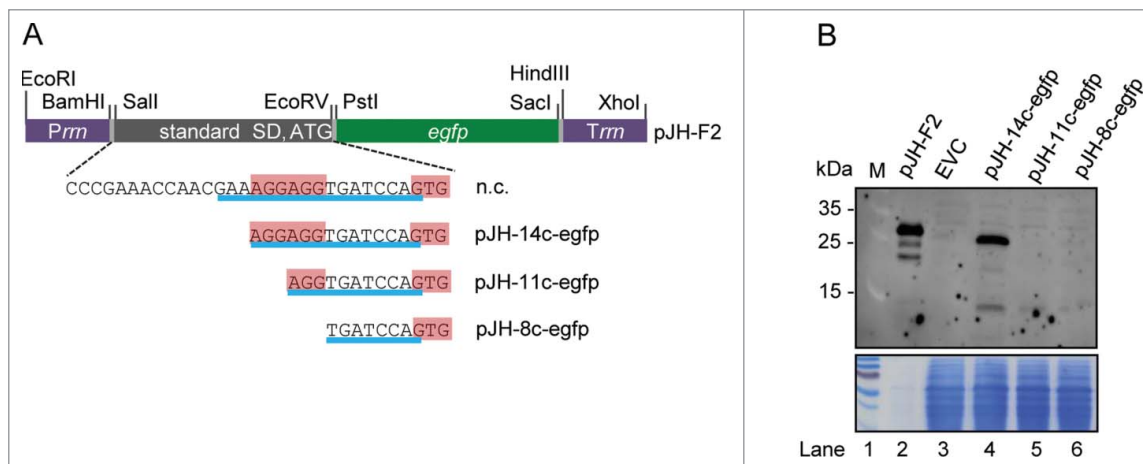


**Figure 5.** Analysis of the influence of truncated *rreB* 5'-UTRs on EGFP translation. (A) Schematic representation of plasmid pJH-F2 and of its derivatives pJH-14c-egfp, pJH-11c-egfp, and pJH-8c-egfp, which contain *rreB-egfp* translational fusions. The standard SD and the ATG start codon of pJH-F2 were replaced by the indicated *rreB* sequences. n.c., cloning of a construct with the full *rreB* 5'-UTR without the *rreB* sORF failed. *Prrm* and *Trm*, see Fig. 4A. (B) Western blot analysis with GFP-specific antibodies of strains containing the indicated constructs (see A). EVC, strain containing plasmid pJH-O1. The bottom panel shows a Coomassie Blue stained SDS-polyacrylamide gel after electrophoresis visualizing the loaded protein amounts. Migration of marker proteins (M) in the gel is indicated at the left side in kDa.

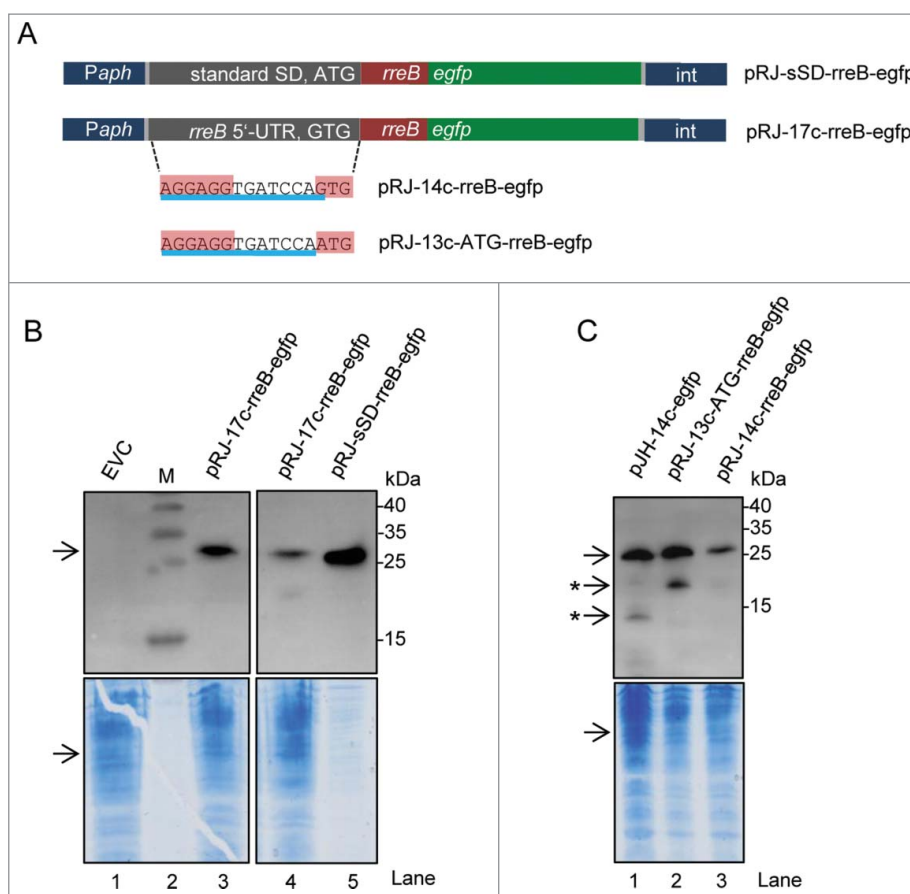


**Figure 6.** The mRNA *rreB* is weakly translated in *B. japonicum*. (A) Schematic representation of the used constructs cloned between a *Paph* promoter and a sequence for integration of the plasmids into the chromosome (*int*).<sup>29</sup> The *rreB-egfp* fusion is preceded either by a standard SD and an ATG start codon (pRJ-sSD-rreB-egfp) or by the full-length 5'-UTR of *rreB* with the 17c-region and the GTG start codon (pRJ-17c-rreB-egfp). Further modifications of the 5'-UTR of *rreB* resulting in pRJ-14c-rreB-egfp and pRJ-13c-ATG-rreB-egfp are indicated on the bottom. (B) and (C) Western blot analysis with GFP-specific antibodies of strains containing the indicated constructs (see A). EVC, plasmid pJPaph-MCS was integrated into the chromosome. Schematic representation of pJH-14c-GTG-egfp is given in Fig. 5A. The bottom panel shows a Coomassie Blue stained SDS-polyacrylamide gel after electrophoresis visualizing the loaded protein amounts. Migration of marker proteins (M) is indicated (in kDa). Arrows indicate the position of the RreB-EGFP band; arrows with asterisks indicate putative degradation products.

90% of the positive control cells harboring pRJ-sSD-rreB-egfp were fluorescent, in cultures with pRJ-17c-rreB-egfp there were almost no fluorescent cells (not shown). To test whether the fusion protein RreB-EGFP accumulates only in a small sub-population, the strain harboring pRJ-17c-rreB-egfp was analyzed additionally by flow cytometry. For thresholding we used an empty vector control (EVC) strain containing chromosomally integrated pRJPaph-MCS as reference and for the adjustment of the gating strategy. No significant difference was detected between cultures of the EVC and the pRJ-17c-rreB-egfp containing strain, both showing 0.03% fluorescent cells (Fig. S8). The fluorescence of those cells was weak and probably represents auto-fluorescence. Single fluorescent and non-fluorescent cells were spotted onto agar plates using FACS. RreB-EGFP was detected by Western blot analysis with GFP-specific antibodies in all cultures originating from single cell isolates with pRJ-17c-rreB-egfp and the signals were of similar intensities (Fig. S8). Altogether, these results suggest that the level of the fusion protein RreB-EGFP is very low in the cells and therefore its fluorescence is under the limit of detection.

To analyze the impact of the GTG codon on *rreB* translation, we constructed a pRJ-14c-rreB-egfp plasmid with the GTG start codon and a mutated derivative pRJ-13c-ATG-rreB-

egfp in which the GTG codon was replaced by ATG (Fig. 6A). Western blot analysis revealed that the ATG codon mediates higher translation efficiency than the GTG codon (compare lanes 2 and 3 in Fig. 6C).

Based on the above data, we conclude that the sORF *rreB* is translated, but its translation is very weak due to the extremely extended SD and the GTG codon.

#### The start codon is important for *rreB* turn-over

In the course of our analyses, we constructed a GUG/UAG mutant of the overexpressed *17c-rreB* RNA (see Fig. 4A), in which the start codon GUG is replaced by the stop codon UAG. This derivative named *16c-rreB*(GUG/UAG) was localized predominantly in the P100 fraction (Fig. 7A), suggesting that it binds to ribosomes with similar efficiency like *17c-rreB* or endogenous *rreB*. However, the *16c-rreB* (GUG/UAG) transcript accumulated to higher levels in the cells than *17c-rreB* (not shown). Since both RNAs are transcribed from the *rrn* promoter, this observation suggested that *16c-rreB*(GUG/UAG) is more stable than *17c-rreB*, pointing to a function of the ribosome in *rreB* degradation. We performed stability measurements and found that the

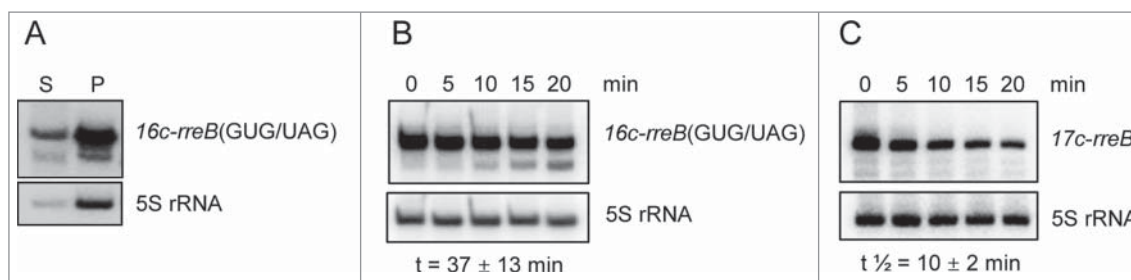


**Figure 7.** The *rreB* start codon is important for the turnover of the small mRNA. Northern blots hybridized with probes directed against the *rreB* sORF and the control 5S rRNA are shown. (A) The *16c-rreB*(GUG/UAG) transcript is localized predominantly in the P100 fraction. (B) and (C) RNA was isolated from cells harvested at the indicated time (min) after stop of transcription by rifampin addition to cultures at an  $OD_{600}$  of 0.5. Stabilities of the overproduced *rreB* derivatives *16c-rreB*(GUG/UAG) and *17c-rreB* were calculated from 4 biological experiments and are given below the panels.

GUG/UAG mutation significantly increased the half-life of the transcript from  $10 \pm 2$  min to  $37 \pm 13$  min (Fig. 7B and 7C). Thus, either formation of 30S initiation complex or 70S ribosome are involved in degradation of *17c-rreB*, suggesting an additional regulatory role of the ribosome in *rreB* expression.

### Similar small genes in other $\alpha$ -proteobacteria

Assuming that the 17 nt complementarity to the 3'-end of 16S rRNA is a hallmark of *rreB* and its functional homologs, we used a 20 nt query corresponding to the 3'-end of 16S rRNA for a BLASTN search in bacterial genomes. We found putative *rreB* analogs containing a 16 nt or 17 nt region of complementarity to the 3'-end of 16S rRNA in many representatives of *Caulobacterales*, *Rhizobiales*, *Rhodobacterales*, and *Rhodospirillales*. It is noteworthy that in contrast to other  $\alpha$ -proteobacteria, in *Azospirillum* the *rre* gene is located on a plasmid and the sORF starts with an ATG. Although the genomic context of *rreB* (Fig. 1A) is quite conserved in *Bradyrhizobiaceae*, it is not conserved in other  $\alpha$ -proteobacteria.

Fig. 8 shows the conservation of the small genes named *rreR* in the *Rhodobacter/Roseobacter* clade. In all cases the last nucleotide of the large complementarity region belongs to a GTG start codon of a sORF comprising 18 codons. There is no sequence similarity between the small proteins RreB and RreR, but they are well conserved in the respective phylogenetic clades (see Fig. 2B, Fig. S1, and Fig. 8B). RreR from *Dinoroseobacter shibae* DFL12 (18 aa) (Fig. 8C) was also synthesized and analyzed by CD- and 1D-NMR spectroscopy. However, similarly to RreB, RreR remained largely unstructured in solution (Figs S9 to S12).

### Discussion

In this work we identified a small mRNA named *rreB* with an extraordinary extended SD (17c-region) in *B. japonicum* and found that it is highly conserved in the family *Bradyrhizobiaceae*. The conservation of an exceptional SD followed by sORF in many bacteria beyond *Bradyrhizobiaceae* shows evolutionary pressure for maintenance of such arrangement. However, so far the function of *rre* genes remains elusive. The similar growth of the EVC and *B. japonicum* which overproduces the ribosome-binding *17c-rreB* mRNA suggests that simple recruitment of ribosomes for preventing translation is

not a major function of *rreB*. This result can be explained by the much higher number of ribosomes when compared with native and overexpressed *rreB* mRNA, as judged from intensity signals in Northern blot hybridizations (data not shown). Further, putative overproduction of the small protein RreB in the strain harboring *pJH-14c* did not influence growth, thus preventing further analysis of its physiological role.

The secondary structure prediction of *rreB* suggested that only the 5' 5' nucleotides of the 17c-region are single-stranded and thus accessible for ribosome binding, while the downstream nucleotides are involved in a conserved hairpin structure (Fig. 2D). We suggest that the predicted single-stranded part of the 17c-region probably functions as a seed region for interaction with 16S rRNA, leading to subsequent melting of the first stem-loop of *rreB* and binding to the 30S ribosomal subunit. This assumption would explain the efficient binding of *rreB* and its *17c-rreB* derivative to ribosomes (as shown by their predominant localization in the P100 fraction) as well as the much lower proportion of *14c-rreB* RNA in P100 (see Fig. 4). The last transcript should harbor only 2 nt in the single-stranded region for seed interaction with 16S rRNA and thus it can be expected that its binding to ribosomes is inefficient.

It is noteworthy that when expressed in *E. coli* (Fig. 4), *rreB* was weakly associated with ribosomes (Fig. S6), pointing to differences in the accessibility of its RBS in the 2 bacterial species. Due to small differences between the 16S rRNA sequences of *B. japonicum* and *E. coli*, the region of complementarity between *E. coli* 16S rRNA and *rreB* is 14 nt with a potential seed interaction region of 3 nucleotides. The latter could be a reason for the inefficient interaction between *rreB* and ribosomes in *E. coli*.

A 17 bp duplex formation between *rreB* and 16S rRNA would encompass the entire single-stranded 3'-end of 16S rRNA in *B. japonicum*. A previous crystallography study with an artificial RNA has shown that 5 nt downstream of the canonical SD can be involved in the formation of the SD helix, which in that case had a length of 12 bp and involved almost all nucleotides of the single-stranded 3'-end of 16S rRNA of *Thermus thermophilus*.<sup>38</sup> Our data revealed important roles for the 9 5' nucleotides of the 17c-region: the 5'-extension upstream of the canonical 6 nt SD AGGAGG was crucial for the highly efficient *rreB* binding to ribosomes (Fig. 4) and the full canonical SD was needed for *rreB* translation (compare lane 4 to lane 5 in Fig. 5). Furthermore, the data suggest that the 8 3' nucleotides of the 17c-region (the 7 nt between the canonical SD and the



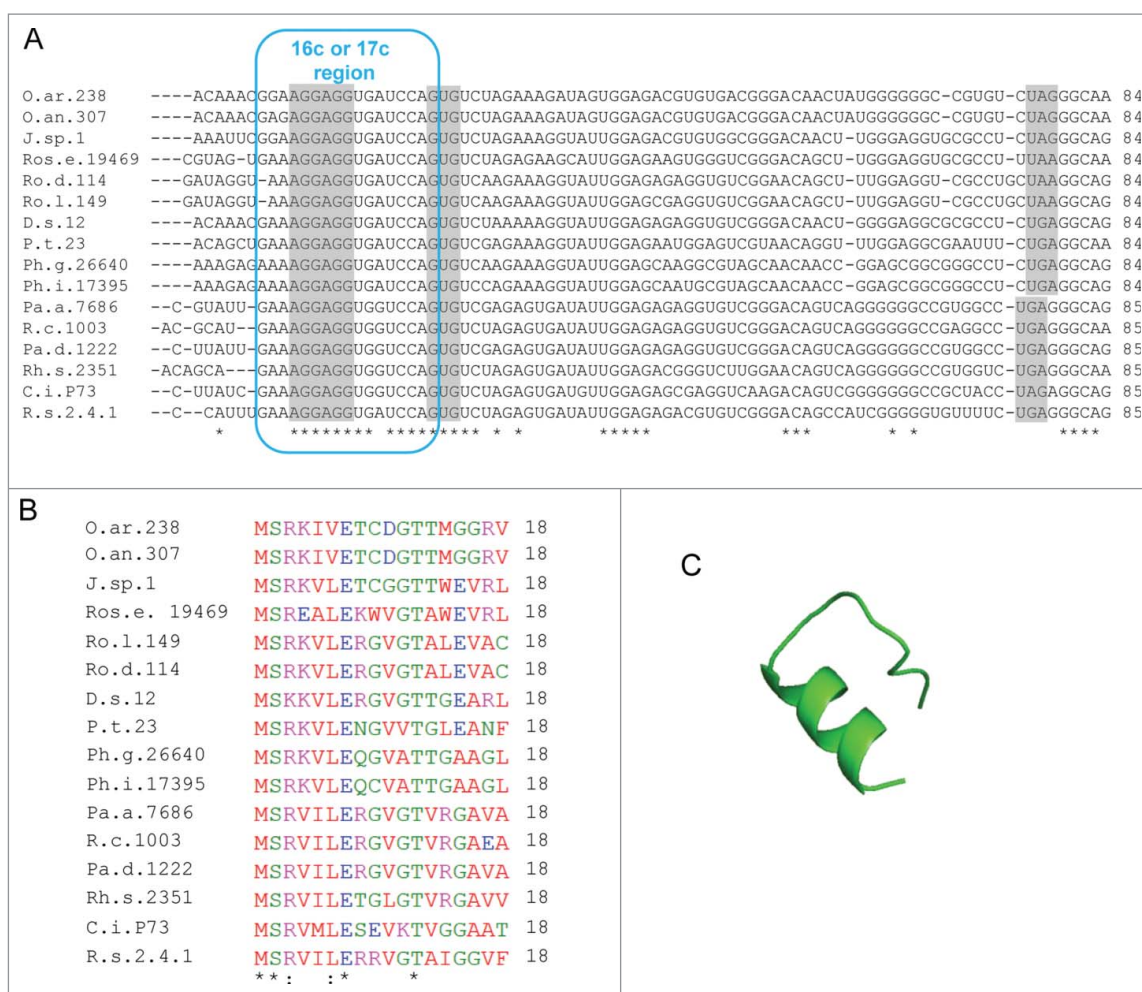


**Figure 8.** Putative *rreB* homologs in *Rhodobacterales*. (A) Multiple sequence alignment of sequences corresponding to the putative small mRNAs containing homologous sORFs of 18 codons (named *rreR*) and preceded by a region with extended complementarity to the 3'-end of 16 sRNA (Extended SD region). Canonical SD, GTG start codon and stop codons are highlighted in gray. For other descriptions see (Fig. 2A). (B) Multiple sequence alignment of the small proteins RreR encoded by the sORFs shown in A). O.ar.238, *Octadecabacter arcticus* 238; O.an.307, *Octadecabacter antarcticus* 307; J.sp.1, *Jannaschia* sp CCS 1; Ros.e.19469, *Roseibacterium elongatum* DSM 19469; Ro.d.114, *Roseobacter denitrificans* OCh 114; Ro.l.149, *Roseobacter litoralis* OCh 149; D.s.12, *Dinoroseobacter shibae* DFL 12; P.t.23, *Planctomarina temperata* RCA 23; Ph.g.26640, *Phaeobacter gallaeciensis* DSM 26640; Ph.i.17395, *Phaeobacter inhibens* DSM 17395; Pa.a.7686, *Paracoccus aminophilus* JCM 7686; R.c.1003, *Rhodobacter capsulatus* SB 1003; Pa.d.1222, *Paracoccus denitrificans* PD 1222; Rh.s.2351, *Rhodovulum sulfidophilum* DSM 2351; C.i.P73, *Celeribacter indicus* strain P73; R.s.2.4.1., *Rhodobacter sphaeroides* ATCC 2.4.1. (C) Predicted spatial structure of RreR from *D. shibae* DFL 12.

start codon, and the first nucleotide of the start codon) serve to minimize *rreB* translation: contrary to our expectations, the *11c-egfp* mRNA harboring AGG was not translated and the *14c-egfp*-mRNA with canonical SD was translated very weakly when compare with the construct with standard SD (Fig. 5).<sup>6,10</sup> Finally, the GTG start codon was identified as an additional determinant keeping *rreB* translation low (Fig. 6C). Thus, our results show that the unique 17c-region enables very efficient binding of *rreB* to ribosomes but keeps its translation weak. It is not clear whether translation is weak under all conditions or *rreB* it is efficiently translated under specific, yet unknown conditions.

The *rreB* stability was dependent on the start codon (Fig. 7), suggesting that *rreB* degradation depends either on the 30S initiation complex or on the 70S ribosome. We favor the latter possibility, since it is known that mRNA is cleaved in ribosomes stalled due secondary structure roadblocks.<sup>39</sup> Strong binding of *rreB* mRNA to 16S rRNA that prevents elongation would result in a similarly trapped ribosome and may lead to *rreB* cleavage and ribosome rescue.

We used the unusually extended complementarity of *rreB* to 16S rRNA to search for similar or similarly regulated genes in other bacteria and detected putative *rre* genes in many  $\alpha$ -proteobacteria. The high similarity between the RBS of *rreB* and of other  $\alpha$ -proteobacterial *rre* mRNAs suggests strong interaction with ribosomes and similar posttranscriptional regulation at the level of degradation and translation. This shows how features of non-translated regions may help to uncover new genes for small proteins without detectable homology at the amino acid sequence level. The conservation of the *rreB* sORF in *Bradyrhizobiaceae*, the *rreR* sORF in *Rhodobacterales* and *rre* sORFs in other  $\alpha$ -proteobacterial lineages suggests that these small genes are important for survival of many  $\alpha$ -proteobacteria.

### Author contributions

J.H and S.T. characterized experimentally *rreB*, E.E.H., A.M. and S.T. performed bioinformatic analyses, R.F.v.B. performed flow cytometry and FACS, N.K. and H.S. performed CD and NMR spectrometry, J.H., E.K., H.S., and E.E.H. wrote the manuscript, E.E.H. conceived the study. All authors read and approved the final manuscript.

## Disclosure of potential conflicts of interest

No potential conflicts of interest were disclosed.

## Acknowledgments

We are grateful to Florian Rossmann and Kai Thormann (University of Giessen) for help with fluorescence microscopy, and to Julia Frunzke (Forschungszentrum Jülich) for support with flow cytometry and FACS. We also thank Saina Azarderakhsh and Franziska Kranz (University of Giessen) for help in some experiments and Hans-Martin Fischer (ETH Zürich) for providing soybean nodules.

## Funding

This work was supported by the Deutsche Forschungsgemeinschaft (DFG) under grant Ev42/4-2 (to E.E.H.); and the Russian Scientific Foundation under grant N 14-24-00061 (to A. M. and E. K; Fig. 1, Fig. 8 and Fig. S1). J. H. was member of IRTG 1384 “Enzymes and multienzyme complexes acting on nucleic acids” supported by the DFG. Work at BMRZ is supported by state of Hesse. H.S. is member of the DFG-funded cluster of excellence: macromolecular complexes.

## ORCID

Sebastian Thalmann  <http://orcid.org/0000-0001-7021-1741>

Elena Evguenieva-Hackenberg  <http://orcid.org/0000-0001-7270-3168>

## References

- Sharma CM, Vogel J. Differential RNA-seq: the approach behind and the biological insight gained. *Curr Opin Microbiol* 2014; 19:97-105 PMID:25024085; <https://doi.org/10.1016/j.mib.2014.06.010>
- Prasse D, Thomsen J, De Santis R, Muntel J, Becher D, Schmitz RA. First description of small proteins encoded by sRNAs in *Methanoscarcina mazei* strain Gö1. *Biochimie* 2015; 117:138-48; PMID:25890157; <https://doi.org/10.1016/j.biochi.2015.04.007>
- Storz G, Wolf YI, Ramamurthi, KS Small proteins can no longer be ignored. *Annu Rev Biochem* 2014; 83:753-77; PMID:24606146; <https://doi.org/10.1146/annurev-biochem-070611-102400>
- Gimpel M, Heidrich N, Mäder U, Krügel H, Brantl S. A dual-function sRNA from *B. subtilis*: SR1 acts as a peptide encoding mRNA on the *gapA* operon. *Mol Microbiol* 2010; 76:990-1009; PMID:20444087; <https://doi.org/10.1111/j.1365-2958.2010.07158.x>
- Shine J, Dalgarno L. The 3'-terminal sequence of *Escherichia coli* 16S ribosomal RNA: complementarity to nonsense triplets and ribosome binding sites. *Proc Natl Acad Sci U S A* 1974; 71:1342-6; PMID:4598299; <https://doi.org/10.1073/pnas.71.4.1342>
- Omatajo D, Tate T, Cho H, Choudhary M. Distribution and diversity of ribosome binding sites in prokaryotic genomes. *BMC Genomics* 2015; 16:604; PMID:26268350; <https://doi.org/10.1186/s12864-015-1808-6>
- Warren AS, Archuleta J, Feng WC, Setubal JC. Missing genes in the annotation of prokaryotic genomes. *BMC Bioinformatics* 2010; 11:131; PMID:20230630; <https://doi.org/10.1186/1471-2105-11-131>
- Kuroda H, Suzuki H, Kusumegi T, Hirose T, Yukawa Y, Sugiura M. Translation of *psbC* mRNAs starts from the downstream GUG, not the upstream AUG, and requires the extended Shine-Dalgarno sequence in tobacco chloroplasts. *Plant Cell Physiol* 2007; 48:1374-78; PMID:17664183; <https://doi.org/10.1093/pcp/pcm097>
- Komarova AV, Tchufistova LS, Supina EV, Boni IV. Protein S1 counteracts the inhibitory effect of the extended Shine-Dalgarno sequence on translation. *RNA* 2002; 8:1137-47; PMID:12358433; <https://doi.org/10.1017/S1355838202029990>
- Osterman IA, Evfratov SA, Sergiev PV, Dontsova OA. Comparison of mRNA features affecting translation initiation and reinitiation. *Nucleic Acids Res* 2013; 41:474-86; PMID:23093605; <https://doi.org/10.1093/nar/gks989>
- Ramamurthi KS, Storz G. The small protein floodgates are opening; now the functional analysis begins. *BMC Biol* 2014; 12:96; PMID:25475548; <https://doi.org/10.1186/s12915-014-0096-y>
- Tenson T, DeBlasio A, Mankin A. A functional peptide encoded in the *Escherichia coli* 23S rRNA. *Proc Natl Acad Sci U S A* 1996; 93:5641-6; PMID:8643630; <https://doi.org/10.1073/pnas.93.11.5641>
- Edwards A, Frederix M, Wisniewski-Dyé F, Jones J, Zorreguieta A, Downie JA. The *cin* and *rai* quorum-sensing regulatory systems in *Rhizobium leguminosarum* are coordinated by ExpR and CinS, a small regulatory protein coexpressed with CinI. *J Bacteriol* 2009; 191:3059-67; PMID:19270098; <https://doi.org/10.1128/JB.01650-08>
- Vogel J, Argaman L, Wagner EG, Altuvia S. The small RNA IstR inhibits synthesis of an SOS-induced toxic peptide. *Curr Biol* 2004; 14:2271-6; PMID:15620655; <https://doi.org/10.1016/j.cub.2004.12.003>
- Fozo EM, Kawano M, Fontaine F, Kaya Y, Mendieta KS, Jones KL, Ocampo A, Rudd KE, Storz G. Repression of small toxic protein synthesis by the Sib and OhsC small RNAs. *Mol Microbiol* 2008; 70:1076-93; PMID:18710431; <https://doi.org/10.1111/j.1365-2958.2008.06394.x>
- Lewis K. Persister cells. *Annu Rev Microbiol* 2010; 64:357-72; PMID:20528688; <https://doi.org/10.1146/annurev.micro.112408.134306>
- Desbrosses GJ, Stougaard J. Root nodulation: a paradigm for how plant-microbe symbiosis influences host developmental pathways. *Cell Host Microbe* 2011; 10:348-58; PMID:22018235; <https://doi.org/10.1016/j.chom.2011.09.005>
- Fischer HM. Genetic regulation of nitrogen fixation in rhizobia. *Microbiol Rev* 1994; 58:352-86; PMID:7968919.
- Čuklina J, Hahn J, Imakaev M, Omasits U, Förstner KU, Ljubimo, N, Goebel M, Pessi G, Fischer HM, Ahrens CH, et al. Genome-wide transcription start site mapping of *Bradyrhizobium japonicum* grown free-living or in symbiosis - a rich resource to identify new transcripts, proteins and to study gene regulation. *BMC Genomics* 2016; 17:302; PMID:27107716; <https://doi.org/10.1186/s12864-016-2602-9>
- Kaneko T, Nakamura Y, Sato S, Minamisawa K, Uchiumi T, Sasamoto S, Watanabe A, Idesawa K, Iriguchi M, Kawashima K, et al. Complete genomic sequence of nitrogen-fixing symbiotic bacterium *Bradyrhizobium japonicum* USDA110. *DNA Res* 2002; 9:189-97; PMID:12597275; <https://doi.org/10.1093/dnares/9.6.189>
- Regensburger B, Hennecke H. RNA polymerase from *Rhizobium japonicum*. *Arch Microbiol* 1983; 135:103-9; PMID:6639271; <https://doi.org/10.1007/BF00408017>
- Delamuta JR, Ribeiro RA, Ormeño-Orrillo E, Melo IS, Martínez-Romero E, Hungria M. Polyphasic evidence supporting the reclassification of *Bradyrhizobium japonicum* group Ia strains as *Bradyrhizobium diazoefficiens* sp. nov. *Int J Syst Evol Microbiol*. 2013; 63:3342-51; PMID:23504968; <https://doi.org/10.1099/ijss.0.049130-0>
- Mesa S, Hauser F, Friberg M, Malaguti E, Fischer HM, Hennecke H. Comprehensive assessment of the regulons controlled by the FixLJ-FixK2-FixK1 cascade in *Bradyrhizobium japonicum*. *J Bacteriol* 2008; 190:6568-79; PMID:18689489; <https://doi.org/10.1128/JB.00748-08>
- Yanisch-Perron C, Vieira J, Messing J. Improved M13 phage cloning vectors and host strains: nucleotide sequences of the M13mp18 and pUC19 vectors. *Gene* 1985; 33:103-19; PMID:2985470; [https://doi.org/10.1016/0378-1119\(85\)90120-9](https://doi.org/10.1016/0378-1119(85)90120-9)
- Simon R, Priefer U, Pühler A. A broad host range mobilization system for *in vivo* genetic engineering: transposon mutagenesis in gram-negative bacteria. *Biotechnology* 1982; 1:784-91; <https://doi.org/10.1038/nbt1183-784>
- Sambrook J, Fritsch EF, Maniatis T. *Molecular cloning: A laboratory manual*. 2nd ed. Cold Spring Harbor Laboratory Press, Cold Spring Harbor, NY, 1989.
- Alvarez-Morales A, Betancourt-Alvarez M, Kaluza K, Hennecke, H. Activation of the *Bradyrhizobium japonicum* *nifH* and *nifDK* operons is dependent on promoter-upstream DNA sequences. *Nucleic Acids Res* 1986; 14:4207-27; PMID:3086837; <https://doi.org/10.1093/nar/14.10.4207>
- Rudolph G, Semini G, Hauser F, Lindemann A, Friberg M, Hennecke H, Fischer HM. The Iron control element, acting in positive and negative control of iron-regulated *Bradyrhizobium japonicum* genes, is a target for the Irr protein. *J Bacteriol* 2006; 188:733-44; PMID:16385063; <https://doi.org/10.1128/JB.188.2.733-744.2006>

29. Ledermann R, Bartsch I, Remus-Emsermann MN, Vorholt JA, Fischer HM. Stable Fluorescent and Enzymatic Tagging of *Bradyrhizobium diazoefficiens* to Analyze Host-Plant Infection and Colonization. *Mol Plant Microbe Interact* 2015; 28:959-67; PMID:26035130; <https://doi.org/10.1094/MPMI-03-15-0054-TA>
30. Madhugiri R, Pessi G, Voss B, Hahn J, Sharma CM, Reinhardt R, Vogel J, Hess WR, Fischer HM, Evguenieva-Hackenberg E. Small RNAs of the *Bradyrhizobium/Rhodopseudomonas* lineage and their analysis. *RNA Biol* 2012; 9:47-58; PMID:22258152; <https://doi.org/10.4161/rna.9.1.18008>
31. Madhugiri R, Evguenieva-Hackenberg E. RNase J is involved in the 5'-end maturation of 16S rRNA and 23S rRNA in *Sinorhizobium meliloti*. *FEBS Lett* 2009; 583:2339-42; PMID:19540834; <https://doi.org/10.1016/j.febslet.2009.06.026>
32. Voss B, Hölscher M, Baumgarth B, Kalbfleisch A, Kaya C, Hess WR, Becker A, Evguenieva-Hackenberg E. Expression of small RNAs in *Rhizobiales* and protection of a small RNA and its degradation products by Hfq in *Sinorhizobium meliloti*. *Biochem Biophys Res Commun* 2009; 390:331-6; PMID:19800865; <https://doi.org/10.1016/j.bbrc.2009.09.125>
33. Rheinberger HJ, Geigenmüller U, Wedd M, Nierhaus KH. Parameters for the preparation of *Escherichia coli* ribosomes and ribosomal subunits active in tRNA binding. *Methods Enzymol* 1988; 164:658-70; PMID:3071687; [https://doi.org/10.1016/S0076-6879\(88\)64076-6](https://doi.org/10.1016/S0076-6879(88)64076-6)
34. Altschul SF, Gish W, Miller W, Myers EW, Lipman DJ. Basic local alignment search tool. *J Mol Biol* 1990; 215:403-10; PMID:2231712; [https://doi.org/10.1016/S0022-2836\(05\)80360-2](https://doi.org/10.1016/S0022-2836(05)80360-2)
35. Smith C, Heyne S, Richter AS, Will S, Backofen R. Freiburg RNA Tools: a web server integrating INTARNA, EXPARNA and LOCARNA. *Nucleic Acids Res* 2010; 38:W373-7; PMID:20444875; <https://doi.org/10.1093/nar/gkq316>
36. Larkin MA, Blackshields G, Brown NP, Chenna R, McGettigan PA, McWilliam H, Valentin F, Wallace IM, Wilm A, Lopez R, et al. Clustal W and Clustal X version 2.0. *Bioinformatics* 2007; 23:2947-48; PMID:17846036; <https://doi.org/10.1093/bioinformatics/btm404>
37. Kelley LA, Mezulis S, Yates CM, Wass MN, Sternberg MJ. The Phyre2 web portal for protein modeling, prediction and analysis. *Nat Protoc* 2015; 10:845-58; PMID:25950237; <https://doi.org/10.1038/nprot.2015.053>
38. Yusupova G, Jenner L, Rees B, Moras D, Yusupov M. Structural basis for messenger RNA movement on the ribosome. *Nature* 2006; 444:391-4; PMID:17051149; <https://doi.org/10.1038/nature05281>
39. Liang W, Rudd KE, Deutscher MP. A role for REP sequences in regulating translation. *Mol Cell* 2015; 58:431-9; PMID:25891074; <https://doi.org/10.1016/j.molcel.2015.03.019>
40. Zahn K, Inui M, Yukawa H. Characterization of a separate small domain derived from the 5' end of 23S rRNA of an alpha-proteobacterium. *Nucleic Acids Res* 1999; 27:4241-50; PMID:10518617; <https://doi.org/10.1093/nar/27.21.4241>
41. Evguenieva-Hackenberg E. Bacterial ribosomal RNA in pieces. *Mol Microbiol* 2005; 57:318-25; PMID:15978067; <https://doi.org/10.1111/j.1365-2958.2005.04662.x>